J|A|C|S COMMUNICATIONS

Published on Web 07/13/2010

Nanoscale Positioning of Individual DNA Molecules by an Atomic Force Microscope

Eric A. Josephs[†] and Tao Ye*[,‡]

Schools of Engineering and Natural Sciences, 5200 North Lake Road, University of California, Merced, California 95343

Received May 10, 2010; E-mail: tye2@ucmerced.edu

Abstract: Here we report a method to assemble nanoscale DNA structures with single-molecule precision. This assembly is accomplished by performing nanografting in the presence of short, thiolated DNA strands that have been diluted by a positively charged alkanethiol. The expected number of DNA molecules per patch can be modulated by the application of an electric potential to the surface during patterning. Our ability to position individual DNA within a controlled nanoscale environment and observe these molecules *in situ* will allow us to understand and potentially decouple the heterogeneity caused by the local environment from the intrinsic properties in single-molecule biophysical measurements. Additionally, our approach can potentially be extended to the molecule-by-molecule assembly of larger artificial test structures of nucleic acids or proteins.

The atom-by-atom or molecule-by-molecule assembly of artificial nanostructures using a scanning probe microscope has revealed unprecedented details of atomic-scale surface chemistry and physics under ultra-high vacuum.[1,2] The ability to manipulate single biomolecules promises to enable analogous insights at biologically relevant interfaces, as the nanometer-scale arrangement of molecular components in a living cell underpins an enormous spectrum of biological functions.[3−5] If we can assemble test structures in which proteins and nucleic acids are deterministically arranged with molecular precision, detailed information about how these molecular components work together at the nanoscale can begin to be unraveled, and artificial biomolecular structures with novel functions may emerge.[4,6]

Most existing approaches to biomolecular patterning, such as microcontact printing, dip-pen nanolithography, and nanografting, pattern bundles of oligonucleotide molecules.[7−9] The question of how to pattern biomolecules with *single-molecule precision* remained largely unaddressed until a novel work by Kufer *et al.*[10] The authors used an atomic force microscope (AFM) to pick up oligonucleotides from a depot area and deposit them onto a target area.[10] This manipulation relies on a clever use of the complementary base-pairing interaction between a DNA strand attached to the tip and the DNA strand to be manipulated.[10] However, due to the roughness of the glass surface used and the conformational flexibility of the strands, the transferred oligonucleotide strands could not be imaged directly by atomic force microscopy. Single-molecule fluorescence microscopy and force spectroscopy, used to characterize the positioned DNA strands, do not have the spatial resolution to provide the feedback necessary for positioning arrays of molecules with high precision.[10−12]

In this report, we present a new approach to achieve the goal of positioning individual oligonucleotide strands. The approach builds on nanografting of alkanethiol self-assembled monolayers (SAMs), developed by Liu and co-workers.[13] Nanografting can reliably produce surface features with lateral sizes approaching 10 nm by selectively desorbing molecules in a preformed alkanethiolate SAM on gold and kinetically backfilling the region with a new thiolated molecule (Figure 1A−C).[13] Although in the past, only bundles or clusters of DNA and protein molecules were patterned using this method,[9,14] we here demonstrate that by diluting the DNA with another alkanethiol molecule, aminoundecanethiol (AUT), individual DNA molecules can be patterned in a way that permits *in situ* verification and quantification of the patterned molecules. This ability derives from the design of the nanostructures (Figure 1C), which limits the mobility of the 5′-thiolated DNA molecules (DNA-SH) on the surface both through direct chemisorption of the thiol to the gold substrate and by electrostatically "pinning" the DNA atop the positively charged AUT SAM, permitting molecular resolution of the DNA using AFM. Moreover, we are able to modulate the average number of DNA per patch by applying an electrochemical potential during nanografting. Our technique provides for controlled DNA−surface interactions due to the significantly more uniform morphology and chemical functionality afforded by SAMs. By reducing variations due to uncontrolled local interactions, such single-molecule structures provide opportunities to understand the conformational changes and reactions of single molecules or small complexes whose dynamics may be obscured in a less controlled or characterized nanoscale environment.[3,15] In addition, patterned single molecules can also serve as a starting point to grow more complex DNA nanostructures on surfaces.[16]

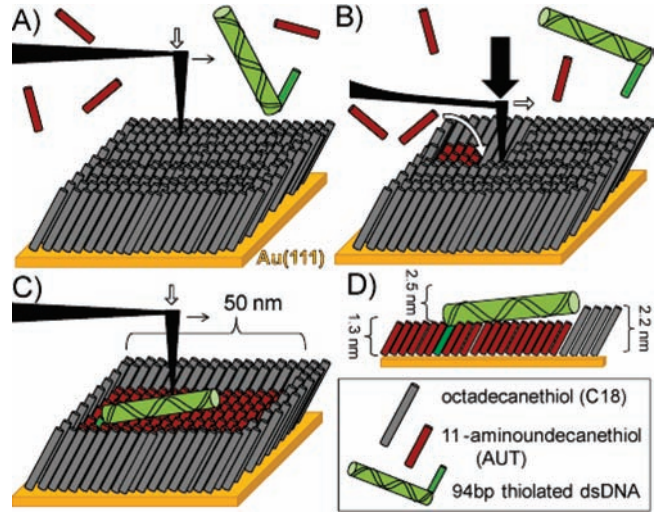

Figure 1. Placement of single chemisorbed DNA molecules on top of a self-assembled monolayer (SAM). (A−C) Protocol for patterning individual DNAs by nanografting. (A) The surface of a pre-assembled monolayer surface is scanned at low force using an AFM. (B) Application of high force by the AFM tip in the presence of a solution containing ∼10000:1 AUT:thiolated DNA molecules results in the local desorption of the SAM and replacement with a monolayer of the solution molecules. (C) The surface may then be immediately imaged using tapping-mode AFM. (D) Expected height profile of DNA assembled atop the AUT patches.

Patterning of DNA molecules onto a preformed SAM of octadecanethiol (C18) by an AFM was performed in a fluidic cell as described

[†] School of Engineering.
[‡] School of Natural Sciences.

10.1021/ja1039677

in Figure 1A−C. Previous reports showed that nanografting with sub-10 μM concentrations of DNA-SH results in sub-monolayer deposition.[9] When we nanografted with 1 μM DNA-SH in 1X Tris acetate EDTA (TAE) solution, no individual DNA structure was resolved by AFM, although the depth of the hole (1.5 nm) was smaller than the thickness of C18 SAM, 2.2 nm (Figure 2A), which indicates a sub-monolayer coverage of DNA molecules.[9] However, the DNA had too much conformational freedom to be individually resolved by AFM. Yet when nanografted in a solution containing an additional equimolar concentration of AUT, a filled-in structure could be imaged (Figure 2B) with heights greater than expected for AUT monolayers alone. Adding 20 times more AUT than DNA resulted in protruding features ~0.5 nm above the background C18 region, which indicates that the DNA was lying directly on the Au(111) surface and embedded within the AUT SAM. Due to the high DNA concentration and ionic strength, these DNA molecules are not dispersed enough to be individually resolved. By decreasing the concentration of the TAE buffer to 0.01X and changing the concentrations of AUT:DNA to ~10 μM:3 nM, we were able to resolve individual rod-like features localized on the 50 nm × 50 nm AUT region (Figures 2C,D and S1 in the Supporting Information).

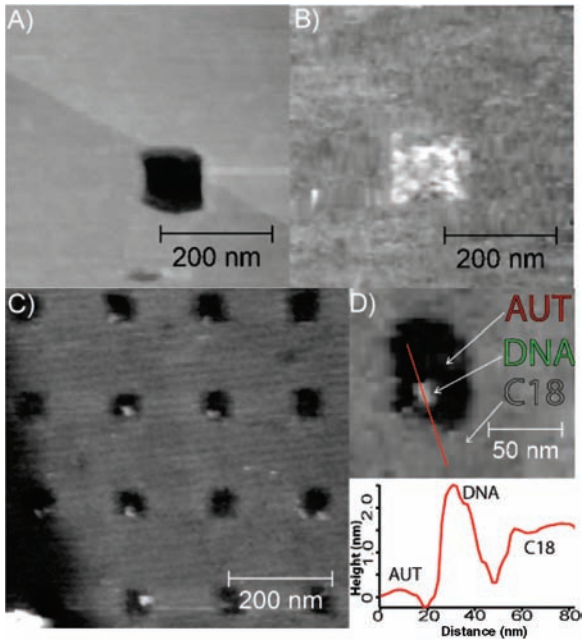

Figure 2. (A−C) Representative images of patches nanografted in solutions containing (A) 1 μM DNA-SH in 1X TAE, (B) 1 μM DNA-SH and 20 μM AUT in 1X TAE, and (C) ~3 nM DNA-SH and 10 μM AUT in 0.01X TAE. Individually resolvable DNA molecules are observed within an array of 50 nm × 50 nm AUT patches by tapping-mode AFM. (D) Single, patterned DNA molecule and height cross-section.

Within the AUT patches, a majority of the protrusions were found to be 2.13 ± 0.44 nm above the AUT layer (Figure 3A), consistent with DNA lying atop the positively charged monolayer[17] (Figure 1D). Control experiments performed by nanografting in a solution containing AUT and DNA with no thiol tether produced only depressed AUT regions, with no protrusions of appropriate heights and lateral sizes (Figure S2 and Table S1, Supporting Information). It appears that under these conditions, the electrostatic attraction alone is not sufficient to immobilize DNA and covalent attachment of the thiolate headgroup to the underlying gold is necessary for surface immobilization. Apart from abnormally large features which were observed in the C18 region due to residual contamination (Figures S1 and S2, Supporting Information), we observe very few molecule-sized protrusions in the C18 matrix. The minimal molecular exchange with the C18 can be attributed to the facts that (i) the DNA concentration is 1000 times

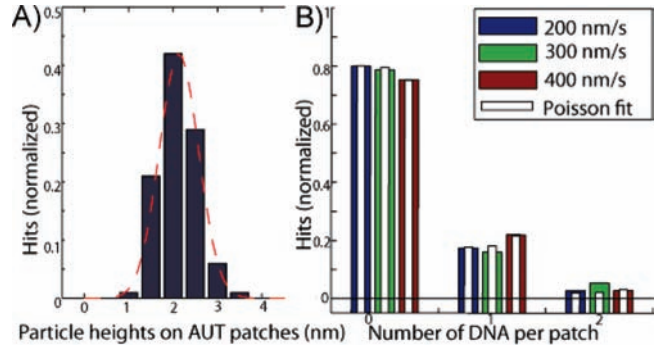

Figure 3. (A) Histogram of the heights of 100 rod-like particles observed on AUT patches, with Gaussian fit. μ = 2.13 nm, σ = 0.44 nm. (B) Histogram of the number of DNA molecules per AUT patch as a function of write speed. Number of DNA per patch follows a Poisson distribution.

lower than the micromolar concentration typically used for nanografting,[9] providing a significantly larger time window to perform nanografting without significant exchange, and (ii) due to the cross section of the oligonucleotide, the DNA-SH does not fit easily into common defects in the C18 SAM such as small single-molecule defects or domain boundaries,[18] reducing the exchange rate. Hence, we conclude that these protrusions correspond to surface-tethered DNA-SH, with the thiol portion anchored to the Au surface and the DNA portion on top of the AUT SAM.

To understand the strength of the DNA−surface interaction, we calculate the degree of ionization $(1 - \beta)$ of the AUT:[19]

$$\log\left(\frac{\beta}{1-\beta}\right) = \mathrm{pH}_\infty + \frac{\psi(0)}{2.303RT/F} - \mathrm{p}K_\mathrm{a}^\mathrm{surf} \qquad (1)$$

where β is the degree of deprotonation of the amine molecules, pH_∞ is the pH of the bulk solution (pH 8.3 in TAE buffer solutions), $\psi(0)$ is the surface potential, R is the ideal gas constant, T is temperature, and F is Faraday's constant. Various measurements have shown that the $\mathrm{p}K_\mathrm{a}^\mathrm{surf}$, the surface acid dissociation constant, of an amine SAM like AUT is only 6−6.5,[20,21] significantly lower than that in the solution.[21] The surface potential is found by using the Gouy−Chapman theory for a charged planar surface, assuming that the monolayer coverage of AUT is 4.55 × 10^{14}/cm^2:[19]

$$\frac{\psi(0)}{2.303RT/F} = 0.863 \sinh^{-1}\left(\frac{7.27(1-\beta)}{\sqrt{8kT\varepsilon_0\varepsilon_\mathrm{r}N_\mathrm{A}C}}\right) \qquad (2)$$

where k is the Boltzmann constant, N_A is Avogadro's number, C is the ionic concentration, and ε_0 and ε_r are the permittivity of a vacuum and the dielectric constant of the imaging solution, respectively. From (1) and (2), we estimate that the AUT layer is less than 0.1% charged at pH 8.3. While additional theoretical studies are required to model the interaction energy between DNA and a nanosized AUT patch, clearly the low degree of ionization contributes to the fact that non-thiolated DNA molecules are not immobilized during nanografting. However, during imaging, the small amount of positive charges reduces the mobility of the covalently tethered DNA, allowing us to verify individual short DNA stands patterned.

We further considered the possibility that the protrusions we observed were actually clusters of DNA packed closer than the resolution of our AFM imaging. We consider this event highly unlikely because of the significant energy cost required for a second DNA to assemble within 10 nm (a worst-case scenario of the AFM resolution) as a result of the electrostatic repulsion between DNA. Under the low ionic concentration used for nanografting DNA, the Debye length was approximately 14.7 nm. We calculated the potential induced by a DNA

assembled atop an AUT layer on a grounded gold surface (Figure S3, Supporting Information) and determined that the electrostatic repulsion energy to assemble a second DNA within 10 nm of the first is 7.3 kT if the second molecule is adsorbed at a angle of 180° with respect to the molecule on the surface. At any other angle, the repulsive energy will be significantly higher, e.g, 17.4 kT at 90°. As no dependence on the nanografting speed in the number of individual DNA molecules patterned at 3 nM DNA-SH concentrations was observed (Figure 3B), we concluded that at this regime, the nanografting process was not diffusion limited. Hence, we assume that the probability of DNA adsorption is controlled by the local concentration of DNA, which is affected by the local electrostatic interaction. We performed a Monte Carlo simulation of nanografting mixed AUT:DNA-SH patches based on the sequential nature of nanografting. We assumed a baseline DNA deposition probability P_0 modified by a Boltzmann factor $\exp[-\phi(r_i)/kT]$ for the electrostatic potential induced by each DNA i already deposited on the surface at a distance r_i from a nanoshaved vacancy (Supporting Information). From these simulations we were able to recreate the roughly Poissonian distribution of the number of DNA per patch we observed experimentally (Figure S4, Supporting Information)[22] and found that less than 6×10^{-4}% of the patterned DNA appeared within 10 nm of another DNA at the ionic concentration used for nanografting, even if we assume the lower limit of the repulsive energy. The results further support that the protrusions we observed were single molecules instead of clusters of DNA.

There are two sources of surface charges: first, the ionization of the AUT SAM and second, the potential-dependent charging of the electric double layer. Hence, we also investigated the effect of surface charges on the assembly of DNA molecules by applying an electrode potential to the Au(111) surface during nanografting (Figure 4). The application of a −200 mV potential (vs Ag/AgCl) resulted in a significant increase in the number of patches observed without DNA. An applied potential of +200 mV (vs Ag/AgCl) conversely increased the number of patches with individual DNA. For the moment, we do not have a quantitative explanation for the surprising linear dependence average number of molecules per patch on the electrode potential (Figure 4, inset). Possible reasons are (1) the electric field at the site of nanografting is highly nonuniform due to the nanoscale geometry and (2) complex kinetics during nanografting is involved. Additional theoretical and experimental investigations are necessary to achieve more quantitative insight. Nevertheless, the results demonstrate that the electrode potential can serve as a convenient handle to modulate the nanografting density without having to change the DNA concentration of the solution. The role of local electrostatic interaction further suggests that a previously assembled DNA would reduce the probability of a second DNA to chemisorb nearby. Monte Carlo simulation results suggest that these electrostatic interactions may be used to optimize the patterning of a single DNA molecule in each nanoscale patch (Figure S4, Supporting Information), which is ideal for single-molecule biophysical experiments.

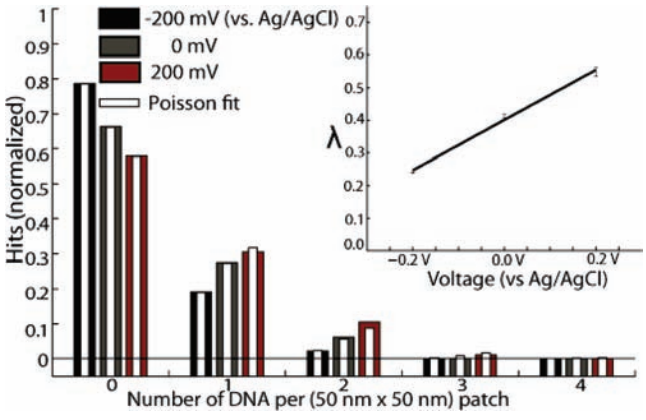

Figure 4. Experimental effects of applied potential during nanografting. Applied negative potential (black) during nanografting results in an increase in DNA squares with no DNA molecules, while application of a positive potential (red) results in an increase of patches with DNA. (Inset) Expected number of DNA per patch (λ) as a function of applied voltage. Error bars were determined by uncertainty of the Poisson fit.

Here we present a method to pattern individual DNA molecules with nanometer resolution. By diluting DNA molecules with another alkanethiol molecule, DNA can be positioned on a chemically well-defined, atomically flat surface and be imaged *in situ*. Additional control of the local interaction and further reduction of the feature size could increase the probability of single-molecule placement. Our approach should retain the versatility of nanografting, such as *in situ* detection and error correction[23] of misplaced DNA molecules and producing multiplexed molecular patterns that are desirable in many studies.[4,6] Since the DNA molecule is confined within a nanografted area, and because both the size and the location of the patches can be controlled with nanometer resolution, nanografting promises to provide high precision for positioning individual DNA molecules and to allow for the assembly of complex biochemical structures on surfaces.

Acknowledgment. We acknowledge support from UC Merced and Petroleum Research Fund. We thank Jingru Shao for assisting with the electrochemical setup, as well as the laboratory of Meng-Lin Tsao for use of their equipment.

Supporting Information Available: Experimental methods, representative AFM images, and simulation details. This material is available free of charge via the Internet at http://pubs.acs.org.

References

(1) Crommie, M. F.; Lutz, C. P.; Eigler, D. M. *Science* **1993**, *262*, 218–220.
(2) Nazin, G. V.; Qiu, X. H.; Ho, W. *Science* **2003**, *302*, 77–81.
(3) Hartwell, L. H.; Hopfield, J. J.; Leibler, S.; Murray, A. W. *Nature* **1999**, *402*, C47–C52.
(4) Collier, J. H.; Mrksich, M. *Proc. Natl. Acad. Sci. U.S.A.* **2006**, *103*, 2021–2025.
(5) Maheshwari, G.; Brown, G.; Lauffenburger, D. A.; Wells, A.; Griffith, L. G. *J. Cell Sci.* **2000**, *113*, 1677–1686.
(6) Dalby, M. J.; Gadegaard, N.; Tare, R.; Andar, A.; Riehle, M. O.; Herzyk, P.; Wilkinson, C. D. W.; Oreffo, R. O. C. *Nat. Mater.* **2007**, *6*, 997–1003.
(7) Xia, Y. N.; Whitesides, G. M. *Annu. Rev. Mater. Sci.* **1998**, *28*, 153–184.
(8) Demers, L. M.; Ginger, D. S.; Park, S. J.; Li, Z.; Chung, S. W.; Mirkin, C. A. *Science* **2002**, *296*, 1836–1838.
(9) Liu, M. Z.; Amro, N. A.; Chow, C. S.; Liu, G. Y. *Nano Lett.* **2002**, *2*, 863–867.
(10) Kufer, S. K.; Puchner, E. M.; Gumpp, H.; Liedl, T.; Gaub, H. E. *Science* **2008**, *319*, 594–596.
(11) Kufer, S. K.; Strackharn, M.; Stahl, S. W.; Gumpp, H.; Puchner, E. M.; Gaub, H. E. *Nature Nanotechnol.* **2009**, *4*, 45–49.
(12) Cordes, T.; Strackharn, M.; Stahl, S. W.; Summerer, W.; Steinhauer, C.; Forthmann, C.; Puchner, E. M.; Vogelsang, J.; Gaub, H. E.; Tinnefeld, P. *Nano Lett.* **2010**, *10*, 645–651.
(13) Liu, G. Y.; Xu, S.; Qian, Y. L. *Acc. Chem. Res.* **2000**, *33*, 457–466.
(14) Staii, C.; Wood, D. W.; Scoles, G. *J. Am. Chem. Soc.* **2008**, *130*, 640–646.
(15) Groves, J. T. *Science STKE* **2005**, *301*, pe45.
(16) Sun, X. P.; Ko, S. H.; Zhang, C. A.; Ribbe, A. E.; Mao, C. D. *J. Am. Chem. Soc.* **2009**, *131*, 13248–13249.
(17) Mou, J. X.; Czajkowsky, D. M.; Zhang, Y. Y.; Shao, Z. F. *FEBS Lett.* **1995**, *371*, 279–282.
(18) Poirier, G. E. *Chem. Rev.* **1997**, *97*, 1117–1127.
(19) Schweiss, R.; Pleul, D.; Simon, F.; Janke, A.; Welzel, P. B.; Voit, B.; Knoll, W.; Werner, C. *J. Phys. Chem. B* **2004**, *108*, 2910–2917.
(20) Fears, K. P.; Creager, S. E.; Latour, R. A. *Langmuir* **2008**, *24*, 837–843.
(21) Wallwork, M. L.; Smith, D. A.; Zhang, J.; Kirkham, J.; Robinson, C. *Langmuir* **2001**, *17*, 1126–1131.
(22) The Poisson distribution suggests that the adsorption of DNA is random and there is no interaction between adsorbed DNA molecules, which seems to contradict the long Debye length. However, Monte Carlo simulation suggests the average number of DNA per patch remains too small to show a significant effect of repulsion between molecules. Simulation suggests that when the average number of DNA is increased beyond one DNA/patch, significant deviation from Poission statistics will be observed.
(23) Xu, S.; Miller, S.; Laibinis, P. E.; Liu, G. Y. *Langmuir* **1999**, *15*, 7244–7251.

JA1039677